Ground- and Excited-State Infrared Spectra of an Azacrown-Substituted $[(bpy)Re(CO)_3L]^+$ Complex: Structure and Bonding in Ground and Excited States and Effects of Ba^{2+} Binding

Jared D. Lewis,[†] Michael Towrie,[‡] and John N. Moore*,[†]

Department of Chemistry, The University of York, Heslington, York, YO10 5DD, United Kingdom, and Central Laser Facility, CCLRC Rutherford Appleton Laboratory, Chilton, Didcot, Oxfordshire, OX11 0QX, United Kingdom

Received: November 28, 2007; In Final Form: January 30, 2008

Ground- and excited-state infrared spectra are reported for a $[(bpy)Re^{I}(CO)_3L]^+$ complex (bpy = 2,2′-bipyridine) in which L contains an azacrown ether that is linked to Re via an amidopyridyl group. Ground-state band assignments are made with the aid of spectra from model complexes in which a similar electron-donating dimethylamino group replaces the azacrown, in which an electron-donor group is absent, and from the L ligands, in conjunction with DFT calculations. Picosecond time-resolved IR (TRIR) spectra in the ν(CO) region show bands characteristic of a metal-to-ligand charge-transfer (MLCT) excited state, $[(bpy^{\bullet-})Re^{II}(CO)_3L]^+$, from the complex in which an electron-donor group is absent, whereas those from the azacrown complex show bands of an MLCT state evolving into those characteristic of a ligand-to-ligand charge-transfer (LLCT) excited state, $[(bpy^{\bullet-})Re^{I}(CO)_3(L^{\bullet+})]^+$, formed upon intramolecular electron transfer. Picosecond TRIR spectra of the azacrown complex in the fingerprint region show strong L ligand bands that indicate that significant charge redistribution occurs within this ligand in the MLCT state and that decay as the LLCT state forms. Picosecond TRIR spectra obtained when Ba^{2+} was complexed to the azacrown show bands of only an MLCT state at all times up to 2 ns, consistent with the presence of Ba^{2+} inhibiting electron transfer from the azacrown N atom to form the LLCT state, and the positions of the bands in the fingerprint region provide direct evidence for the proposal that charge redistribution within the L ligand induces Ba^{2+} release from the azacrown in the MLCT state.

Introduction

We have been studying $[(bpy)Re(CO)_3L]^+$ complexes in which L contains a terminal azacrown ether linked to Re via an amide, alkene, or alkyne group and that can act as metal cation sensors and light-controlled ion switches.[1−7] The amide complex **1** was first reported in 1991 by MacQueen and Schanze,[8] along with model complex **3** in which L does not have a terminal electron-donor group, and their emission studies showed that the metal-to-ligand charge-transfer (MLCT) state lifetime of **1** is <1 ns, whereas that of **3** is ca. 150 ns. They proposed that the MLCT state of **1** is quenched rapidly by intramolecular electron transfer from the azacrown nitrogen to Re to generate a ligand-to-ligand charge-transfer (LLCT) state, and we have reported pico- and nanosecond time-resolved UV−visible absorption (TRVIS) studies that show that forward electron transfer to form the LLCT state occurs in ca. 500 ps (k_{FET}^{-1}) and that back electron transfer to return to the ground state occurs in ca. 19 ns (k_{BET}^{-1}), as shown in Scheme 1.[1]

MacQueen and Schanze showed that binding a metal cation to the azacrown ether to form **1**-M^{n+} lengthens the MLCT-state lifetime, and they proposed that the bound cation inhibits the electron-transfer process;[8] the MLCT lifetime of **1**-M^{n+} was found to be shorter than that of **3** and to depend on the identity of the bound cation, leading to the proposal that a bound cation is released in the MLCT excited state for some metals. We recently investigated this mechanism using nanosecond TRVIS spectroscopy,[2] showing conclusively that release occurs in ca. 5−100 ns for Li^+, Na^+, Ca^{2+}, and Ba^{2+}, with the rate constant (k^*_{off}) decreasing in the order $Na^+ \geq Li^+ > Ba^{2+} > Ca^{2+}$, as illustrated in Scheme 2 for **1**-Ba^{2+}. We also showed that subsequent cation rebinding to the ground state restores the starting thermal equilibrium in ca. 0.1 μs to 1 ms, with the rate constants and detailed mechanism depending on the identity of the cation.

TRVIS measurements provide good kinetic information, and they have enabled the excited states of these systems to be identified and the photophysical and ion-switching mechanisms to be established, but the broad TRVIS bands do not provide detailed information on the changes in structure, bonding, and charge distribution that drive metal cation release upon excitation. Time-resolved vibrational spectroscopy can generally provide such information,[9−11] and the excited states of several $(bpy)Re(CO)_3L$ and related complexes have been studied

[†] The University of York.
[‡] CCLRC Rutherford Appleton Laboratory.

10.1021/jp711260d CCC: $40.75
Published on Web 04/05/2008

SCHEME 1: Photochemical Mechanism for 1

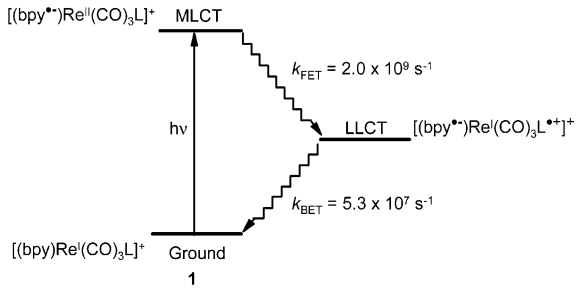

SCHEME 2: Photochemical Mechanism for 1-Ba^{2+}

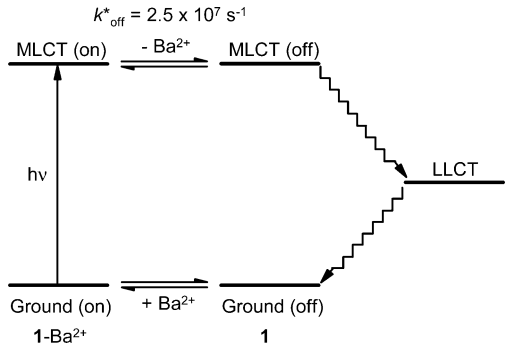

successfully with time-resolved infrared (TRIR) spectroscopy by monitoring shifts in the strong ν(CO) bands upon excitation.[9−22] We have shown that ground-state IR and resonance Raman (RR) spectra report effectively on changes within the L ligand on metal cation binding to the azacrown of $[(bpy)Re(CO)_3L]^+$ complexes with alkene and alkyne linkers,[7] suggesting that time-resolved vibrational spectroscopy may be used to study the changes that drive the ion-release mechanisms in the excited states of such systems.

We recently reported a steady-state and nanosecond transient resonance Raman study of the amide-linked system **1**, its azacrown-bound forms **1**-Li^+, -Na^+, -Ba^{2+}, and -Ca^{2+}, and its models.[3] The ground-state RR spectra generally provided a rich set of bands from both the $(bpy)Re(CO)_3$ group and the L ligand, whereas the excited-state RR spectra generally provided several bpy bands and a single ν(CO) band from the $(bpy)Re(CO)_3$ group, with few bands from the L ligand. The resonance effect enabled spectra from the MLCT and LLCT states to be observed selectively, and the data provided strong support for the proposed ion-switching mechanism as well as information on structure and bonding in these excited states.

Here, we report steady-state infrared spectra of **1**, its azacrown-bound form **1**-Ba^{2+}, the model complexes **2**−**4**, and the L ligands L**1** and L**2**. We assign the ground-state IR bands of **1** by comparison to those of the model complexes and ligands and with the aid of DFT calculations on L**2**. We then report picosecond TRIR spectra of **1**, **3**, and **1**-Ba^{2+}, which we find generally provide a full set of two or three ν(CO) bands from the $(bpy)Re(CO)_3$ group and a rich set of fingerprint-region bands from the L ligand that provide valuable information on the changes that occur within this ligand upon excitation. This TRIR work extends our time-resolved vibrational studies of this system into the picosecond regime, where the MLCT → LLCT conversion occurs (Scheme 1), and it complements our earlier Raman work because it provides information on changes within the L ligand, from bands that were not accessible in those studies. More generally, this study provides a novel example of the application of TRIR spectroscopy to a light-controlled ion-release system, demonstrating how IR bands in both ν(CO) and fingerprint regions can be used report on the charge redistribution that occurs upon excitation and how it is modified when a metal cation is bound to the azacrown.

Experimental Procedures

The ligands and complexes were synthesized according to reported methods[3,8,23] and characterized using ^{1}H NMR and electrospray ionization mass spectrometry, as reported previously.[1−3] Barium perchlorate (Aldrich) was dried overnight under a vacuum at 230 °C, and a large excess was added to a solution of **1** under nitrogen to prepare **1**-Ba^{2+}; UV−vis absorption spectra were recorded to verify full complexation to the azacrown.[2] Steady-state and time-resolved IR spectra were recorded using acetonitrile solvent (Aldrich) because it dissolves both the complexes and the barium perchlorate used to generate **1**-Ba^{2+}; CH_3CN was used for studies in the ν(CO) region (ca. 1800−2100 cm^{-1}), whereas CD_3CN was used for studies in the fingerprint region (ca. 1000−1800 cm^{-1}) because of its much weaker bands. Steady-state IR spectra were also recorded using dichloromethane solvent (Aldrich) because it dissolves all of the ligands and complexes (including L**1** and L**2**, which are only sparingly soluble in acetonitrile), it gives good-quality spectra upon addition of HCl (unlike acetonitrile), and it enables both regions to be studied readily with one solvent because there are only two strong solvent bands (at ca. 1260 and 1425 cm^{-1}); however, the metal perchlorates are not soluble in dichloromethane, precluding studies of the **1**-M^{n+} complexes that are the main target of our work. Where direct comparisons were possible, the steady-state IR spectra from acetonitrile and dichloromethane samples were found to be similar to each other.

Steady-state IR spectra were recorded using a Nicolet Impact 410 FTIR spectrometer, with samples of ligands and complexes at ca. 10^{-2} to 10^{-3} mol dm^{-3} held in a 100 μm path length cell with calcium fluoride windows. The spectra of samples containing barium perchlorate are presented after the scaled subtraction of spectra from barium perchlorate solutions at comparable concentrations, and the spectrum from a sample in acidified dichloromethane is presented after the scaled subtraction of a spectrum from the acidified solvent.

Picosecond TRIR spectra were recorded at the Rutherford Appleton Laboratory, and the instrumentation has been described in detail.[16] Samples at ca. 0.4−1.0 × 10^{-3} mol dm^{-3} were contained in a 100 μm path length cell mounted on an $x-y$ translation stage. They were pumped at 400 nm (ca. 1 μJ energy; ca. 200 fs pulse width; 1 kHz repetition rate; and ca. 300 μm beam diameter), and each experiment involved recording a series of overlapping IR probe windows (ca. 150 cm^{-1} width), with the pump and probe polarizations set at the magic angle (54.7°). The TRIR spectra presented here were obtained by joining adjacent windows, where possible at an appropriate wavenumber where the transient absorption was near the baseline.

DFT calculations were performed with the Gaussian 98 package,[24] using the B3LYP functional and the 6-31G(d) basis set, and output files were parsed and analyzed using the MOLEKEL[25] and MOLDEN[26] packages. The calculated vibrational frequencies were scaled by the recommended factor of 0.9613,[27] and a calculated spectrum was created by applying a 5 cm^{-1} (fwhm) Lorentzian function scaled to the calculated intensity of each band.

Results and Discussion

Ground-State IR Spectra of 1−4. Steady-state IR spectra in the fingerprint region are shown in Figure 1 for **1**, **2**, L**1**, and L**2**, along with the DFT calculated IR spectrum of L**2**, and in

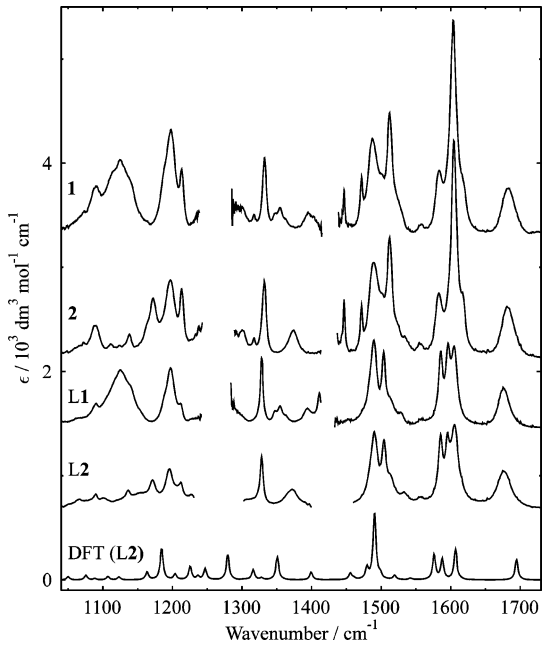

Figure 1. Fingerprint-region IR spectra of **1**, **2**, L**1**, and L**2** in CH_2Cl_2 (regions of strong solvent absorption omitted, and spectra offset for clarity), along with the calculated IR spectrum of L**2**.

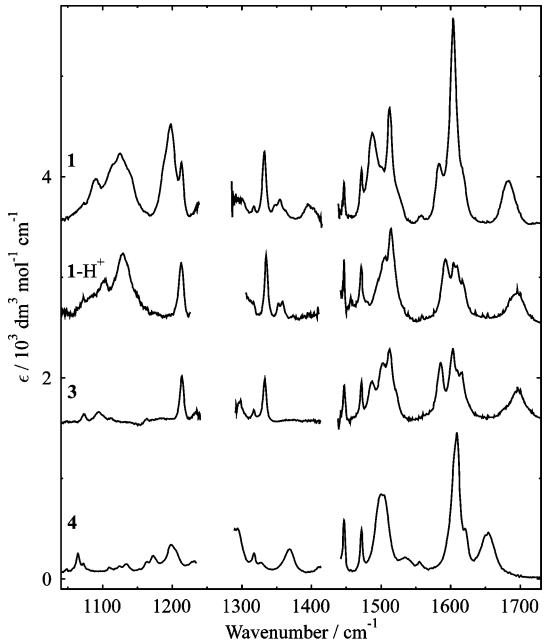

Figure 2. Fingerprint-region IR spectra of **1**, **1**-H^+, **3**, and **4** in CH_2Cl_2 (regions of strong solvent absorption omitted, and spectra offset for clarity).

Figure 2 for **1**, **1**-H^+, **3**, and **4**. Ground-state IR band positions are given in Table 1, including those from the ν(CO) region (spectra of **1** and **3** in this region are included within Figures 6 and 7).

*(bpy)Re(CO)$_3$ Group Bands of **1**−**4***. The ground-state IR spectra of **1**−**4** give bands at ca. 2035 and 1930 cm^{-1} that are assigned to $\nu(CO)_{Re}$ modes (Table 1);[28] the observation of two rather than three bands is attributable to pseudo-C_{3v} symmetry at the Re center, arising from coordination of the L ligand via a pyridyl group.[7,17,29] The close similarity in the pair of $\nu(CO)_{Re}$ bands from **1**−**3** indicates that the variation between the respective azacrown, -NMe_2, and -H substituents at the terminus of the L ligand has a negligible effect on the Re center in the ground state. A set of three relatively narrow and moderately intense IR bands at ca. 1472, 1447, and 1317 cm^{-1} from complexes **1**−**4** but not from ligands L**1** and L**2** (Figures 1 and 2) occurs also for (bpy)Re(CO)$_3$Cl and other [(bpy)Re(CO)$_3$L]$^+$ systems,[7] and they can be assigned readily to modes of the bpy ligand (Table 1).[30,31]

*L Ligand Bands of **1** and **2***. A comparison of the spectra of **1** and **2** with those of L**1** and L**2**, respectively (Figure 1), shows clearly that the remaining bands in the fingerprint region can be assigned to modes of the respective L ligand; these bands dominate the IR spectra in this region. The similarities between these spectra indicate that the band assignments can be based on the relatively simple L**2** ligand, and so its IR spectrum was calculated using DFT with the B3LYP functional and the 6-31G-(d) basis set, consistent with our earlier calculation of its Raman spectrum using this method.[3] This approach has been shown to provide good results for similar donor−acceptor organic compounds;[32] the use of a dimethylamino rather than an azacrown substituent, and the absence of the (bpy)Re(CO)$_3$ group, simplifies the calculations.[7] The calculated IR spectrum of L**2** is shown in Figure 1, and calculated displacement vectors for selected modes that give IR-active bands are shown in Figure 3. The calculations indicate that there is coupling between the various groups within the L ligand because many modes involve the motion of atoms throughout the molecule; some involve vibrations within both phenyl and pyridyl rings, and many involve vibrations of the amide group. However, the calculated coupling between the two rings is generally weaker for this amide ligand than that we reported for the alkene and alkyne analogues,[7] and its relative weakness can be attributed to a small twist between the rings in the amide group, which is not fully planar.[3] Generally, the calculations on L**2** indicate that the same modes give strong bands in both IR and Raman[3] spectra. Table 1 lists assignments that we discuss in detail next; they are based on the calculated IR- and Raman-active modes of L**2**, on a consistent approach to the IR assignments made here and the Raman assignments we made earlier,[3] and on the IR and Raman assignments we have discussed in detail for the alkene and alkyne analogues.[7] Four strong IR bands of the amide ligands and complexes that were not observed for the alkene and alkyne analogues[7] can be assigned to modes involving the amide group.

The moderately strong and relatively broad IR band at ca. 1683 cm^{-1} from **1**, **2**, L**1**, and L**2** is very strong in their RR spectra,[3] and it is assigned unambiguously to an amide I mode,[33−35] which involves amide CO stretching and NH bending and which is calculated at 1695 cm^{-1} for L**2** (Figure 3). Three IR bands at ca. 1600 cm^{-1}, from both ligands and complexes, are readily assigned from the calculated IR spectrum of L**2**: the strong band at ca. 1618 cm^{-1}, observed distinctly for the free ligands and as a shoulder for the complexes, is assigned to a phenyl-centered mode involving Wilson 8a and 9a vibrations calculated at 1607 cm^{-1}; the strong band at ca. 1604 cm^{-1}, which becomes very strong on attachment to the Re group and which was also observed to be very strong in the RR spectra,[3] is assigned to a pyridyl-centered mode involving Wilson 8a and 9a vibrations calculated at 1588 cm^{-1}; and the strong band at ca. 1583 cm^{-1} is assigned to a mode involving NH bending coupled to pyridyl ring Wilson 8b and 3 vibrations calculated at 1576 cm^{-1} (Figure 3). A weak IR band at 1558 cm^{-1} and a weak IR shoulder at ca. 1526 cm^{-1} were observed as moderately strong bands in the RR spectrum of **1**,[3] and they are assigned to phenyl modes involving coupled Wilson 8b and 3 and Wilson 18a and 19a vibrations calculated at 1542 and 1519 cm^{-1}, respectively.

Several weak IR bands are calculated at ca. 1450−1500 cm^{-1}, including alkyl vibrations, and several may contribute to the broad feature observed at ca. 1480−1520 cm^{-1}. An amide II vibration, involving NH bending and CN stretching, typically

TABLE 1: Observed IR Band Positions (cm^{-1}) for Ground and Excited States of 1−4, L1, and L2;[a,b] Calculated Positions for Ground-state L2; and Assignments

1			**1**-Ba^{2+}		**1**-H^+	**2**	**3**		**4**	L**1**	L**2**		assignment	
IR ground	TRIR MLCT	TRIR LLCT	IR ground[b]	TRIR MLCT	IR ground	IR ground	IR ground	TRIR MLCT	IR ground	IR ground	IR ground	DFT ground	L-centered[c]	Re-centered[d]
2035	2069	2010	2035	2073	2035	2035	2035	2073	2036					$\nu(CO)_{Re}$
1930	2010	1901	1930	2020	1932	1931	1931	2014	1932					$\nu(CO)_{Re}$
	1973			1975				1973						$\nu(CO)_{Re}$
1683	1694		1685	1683	1696	1682	1696		1654	1676	1677	1695	ν(CO) + NH bend (amide I)	
1618 sh	1616		1616 sh		1617[e]	1617 sh	1615		1621	1605	1606	1607	8a/9a (ph)	
1604	1599		1605	1593	1604[e]	1605	1603		1609	1596	1596	1588	8a/9a (py)	
1583	1579		1593	1560	1593	1583	1586		1605 sh	1586	1586	1576	NH bend + 8b/3 (py)	
1558						1558			1555	1558	1557	1542	8b/3 (ph)	
1526 sh			1514 sh			1534	1521		1534	1529	1533	1519	18a/19a (ph) + Me + ν(ph−N)	
1512	1497		1507	1492	1514	1512	1512		1505	1504	1504	1490	NH bend + ν(C−N) (amide II) + 18a/19a (py)	
1501 sh					1505	1502 sh	1502							
1487	1461		1492		1506	1489	1487		1500	1490	1490	1480	NH bend + ν(C−N) (amide II) + 18a/19a (py)	
1472			1473		1472	1472	1472		1472					ν_{27} (bpy)
1447			1447		1447	1447	1447		1447					ν_{18} (bpy)
1428[b]	1406		1430									1399	18b/14 (py)	
1395	1383	1290	1299			1374			1369	1394	1372	1351	18a/19a (ph) + ν(ph−N) + Me	
1363					1358					1363			azacrown	
1355			1358		1353					1355			azacrown	
1347										1348			azacrown	
1332	1338		1335	1342	1335	1332	1333		1328	1328	1328	1316	3 (py)	
1317			1318			1317	1317		1318					ν_{29} (bpy)
1301[b]	1308		1299	1303		1300	1298		1294			1305	3 (ph)	
1273[b]			1275									1279	NH bend (amide III) + 18a (py) + 3 (ph)	
1245[b]			1246									1247	18a (py) + 18a (ph) + ν(py−am) + ν(ph−am)	
												1236	Me rock	
1237[b]												1225	NH bend + 9a (py) + 9a (ph)	
1213			1213		1213	1213	1214		1205	1212	1212	1204	9a (py)	
1198			1207			1197			1198	1197	1196	1184	9a (ph)	
1188 sh						1172			1173		1171	1163	Me + 18a/1 (ph)	
1125					1129					1125			azacrown ν(C−O−C)	
1090					1104	1089	1094			1090	1090	1088	18b (py) + NH bend + 18a (ph)	

[a] Positions from ground states in dichloromethane, except where indicated, and from excited states in acetonitrile (CH_3CN or CD_3CN, as indicated in the text). [b] Positions in acetonitrile. [c] Assigned motions given in order of decreasing contribution, generally based on calculations on L**2**, with ph = phenyl, py = pyridyl, and numbers indicating Wilson vibrations. [d] bpy = Bipyridyl, with numbers indicating modes according to ref 30. [e] Small uncertainty in positions and intensities due to a strong overlying solvent band for HCl-acidified dichloromethane.

gives a band at ca. 1510−1550 cm^{-1} that is strong in the IR and weak or absent in the Raman spectrum.[33−35] The calculations here indicate that the amide II vibration of L**2** couples strongly to the pyridyl 18a vibration to give two modes at 1490 and 1480 cm^{-1} arising from in-phase and out-of-phase combinations (Figure 3), with the higher wavenumber band calculated to be the stronger of the two (ca. 6:1) and the strongest band in the IR spectrum (by ca. 2×). We assign two strong IR bands at ca. 1512 and 1487 cm^{-1}, which were not observed in the RR spectra,[3] to these modes; they are of comparable strength to each other and to the other strong bands in the IR spectra.

A moderately strong IR band of **1** at 1428 cm^{-1} (obscured by a solvent band in CH_2Cl_2 but seen in CD_3CN; see Figure 4) is assigned to a mode involving pyridyl 18b and 14 vibrations calculated at 1399 cm^{-1}. The assignment of the other IR bands in this region, at ca. 1340−1400 cm^{-1}, is not straightforward, but it is aided not only by the calculation on L**2** but by similarities with the IR spectra and calculations for the alkene and alkyne systems,[7] as well as those from detailed studies reported for para-dimethylaminobenzonitrile (DMABN) and its isotopomers.[32] A mode involving ph−N stretching is calculated to be strongly mixed with phenyl 18a and 19a and alkyl vibrations for the amide, alkene, and alkyne models, and it is calculated to give a strong IR band at 1351 and 1353 cm^{-1} for the phenyl−NMe_2 systems L**2** and DMABN,[32] respectively. Hence, we assign a moderately strong and broad IR band observed at ca. 1374 cm^{-1} from the -NMe_2 systems **2** and L**2** to this mode, comparable to the assignment of a strong IR band at 1372 cm^{-1} to this mode in DMABN.[32] We assign the equivalent mode from the azacrown systems **1** and L**1** to a moderately strong and broad IR band at ca. 1395 cm^{-1}, comparable to the assignment of similar IR bands at ca. 1395 cm^{-1} from the alkene and alkyne azacrown analogues.[7,36] A band assigned to a mode involving ph−N stretching has been observed at ca. 1350−1400 cm^{-1} in several related donor−acceptor 1,4-disubstituted dialkylaminophenyl systems,[32,37−40] and it has been proposed[32] that its relatively high wavenumber is indicative of ph−N double-bond character arising from significant charge transfer in the ground state. The canonical form of L**1** and L**2** labeled A in Scheme 3 illustrates this proposal, and it may contribute significantly due to the presence of both an azacrown or dialkylamino electron donor and an amido−pyridyl electron acceptor; the calculated structure of L**2** is close to planar at the dimethylamino N atom, consistent with this effect.[3,41]

A moderately strong three-peaked IR band at ca. 1355 cm^{-1} is seen from the azacrown systems **1** and L**1** but not from the dimethylamino systems **2** and L**2**, and it is assigned to azacrown modes because it was also observed from phenyl−azacrown itself.[7] A mode arising from a phenyl 3 vibration calculated at

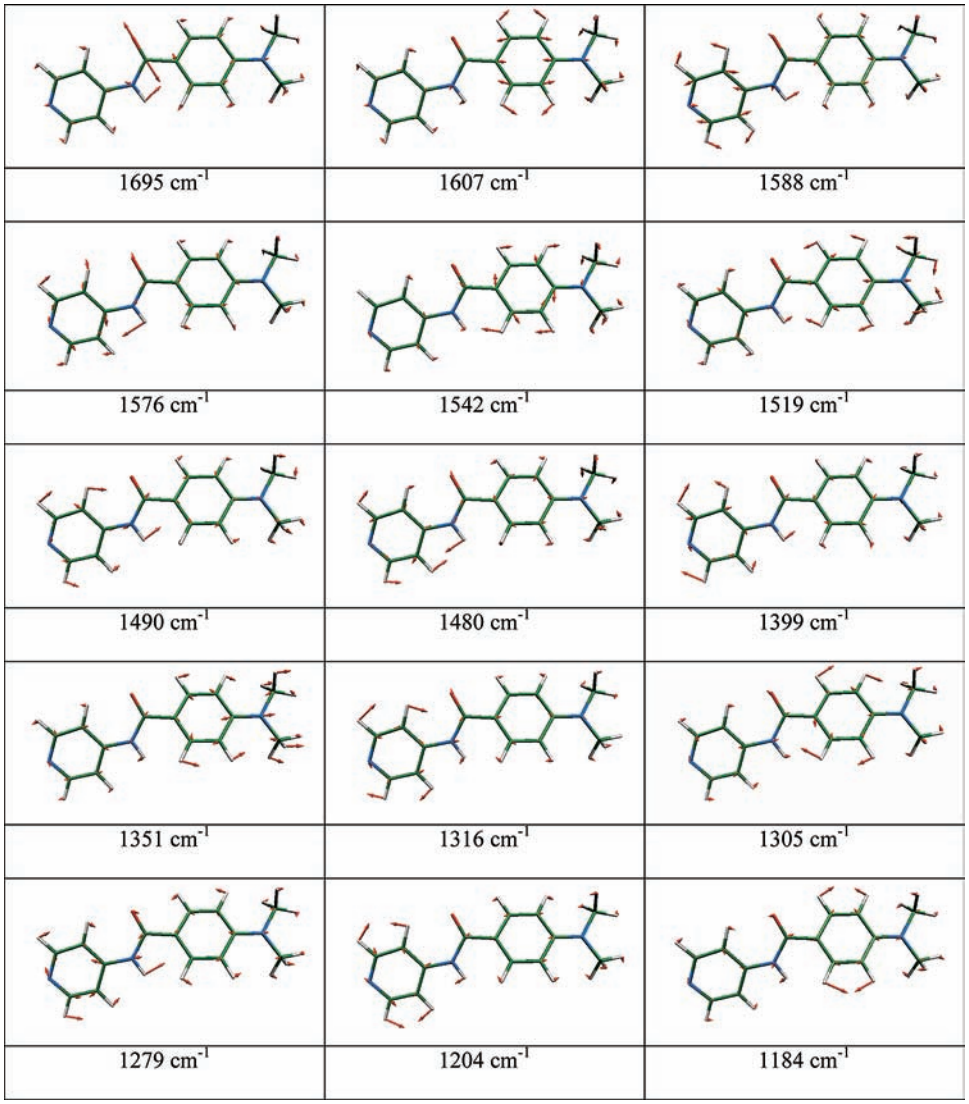

Figure 3. Displacement vectors for selected calculated vibrational modes of L**2**.

SCHEME 3: Canonical Forms of Ligands L1 and L2

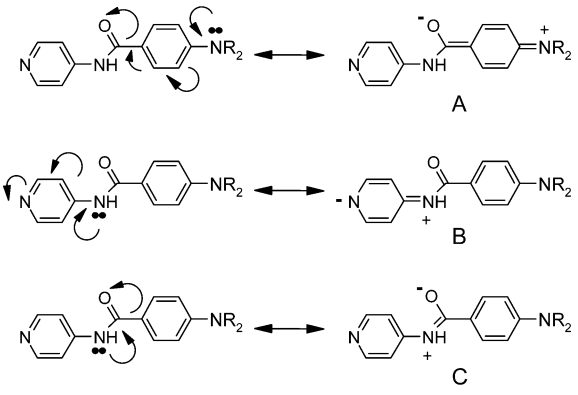

1328 cm^{-1} for L**2** also may contribute to this feature, but no such bands were observed from the dimethylamino models studied here, in contrast to the IR bands at ca. 1350 cm^{-1} observed from the alkene and alkyne diethylamino models that resulted in some bands in this region being assigned to L ligand bands for the respective azacrown systems.[7] A strong IR band at ca. 1332 cm^{-1} from **1** and **2**, and at ca. 1328 cm^{-1} from L**1** and L**2**, is assigned to a calculated mode at 1316 cm^{-1} involving a pyridyl 3 vibration, and a weaker band from **1** at ca. 1301 cm^{-1} (obscured by a solvent band in CH_2Cl_2 but seen in CD_3CN; see Figure 4) is assigned to a calculated mode at 1305 cm^{-1} involving an equivalent phenyl 3 vibration.

An amide III vibration, involving NH bending and CN stretching, typically gives a band at ca. 1250−1300 cm^{-1} in secondary amides that is moderately strong in the IR and strong in the Raman spectrum.[33−35] Our calculations indicate that the amide III vibration of L**2** couples to pyridyl 18a and phenyl 3 vibrations to give a mode at 1279 cm^{-1}, and we assign a strong IR band from **1** at ca. 1273 cm^{-1} (obscured by a solvent band in CH_2Cl_2 but seen in CD_3CN; see Figure 4) that is also strong in the RR spectrum[3] to this mode. Two other weak IR bands seen from **1** in CD_3CN at 1245 and 1237 cm^{-1} are assigned to delocalized modes calculated at 1247 and 1225 cm^{-1} for L**2**, the latter being another mode in this region that involves an NH bending vibration.

Two IR bands at ca. 1213 and 1198 cm^{-1} from **1**, **2**, L**1**, and L**2** are assigned to modes involving 9a vibrations centered on the pyridyl and phenyl rings, respectively, calculated at 1204 and 1184 cm^{-1} for L**2**, and for which matching bands were observed in the RR spectra; the phenyl 9a mode typically gives an intense band at 1100−1200 cm^{-1} in similar compounds.[32,37−40,42] An IR band observed as a shoulder at ca. 1188 cm^{-1} for the

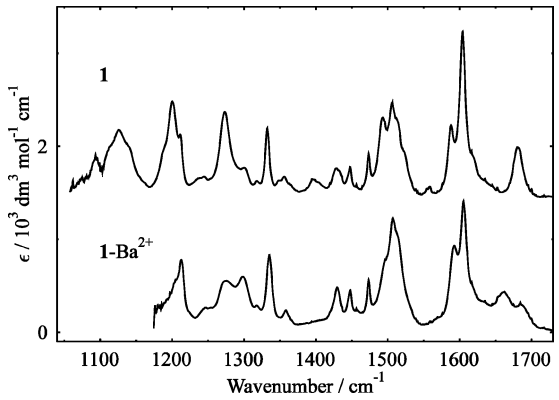

Figure 4. Fingerprint-region IR spectra of **1** and **1**-Ba^{2+} in CD_3CN (regions of strong perchlorate absorption omitted, and spectra offset for clarity).[54]

azacrown systems and as a distinct band at ca. 1172 cm^{-1} for the dimethylamino systems is assigned to a mode involving an alkyl vibration coupled to phenyl 18a and 1 vibrations calculated at 1163 cm^{-1} for L**2**; its position is similar to that reported for other dimethylaminophenyl compounds.[32,37−40,42] The broad band at ca. 1125 cm^{-1} that occurs for the azacrown compounds **1** and L**1** is assigned to ν(C−O−C) modes of the azacrown ring.[43] A moderately strong IR band at ca. 1090 cm^{-1} from **1**, **2**, L**1**, and L**2** is assigned to a calculated mode at 1088 cm^{-1}, in which the pyridyl 18b vibration is coupled to NH bending and phenyl 18a vibrations; a Raman band at 1060 cm^{-1} was assigned to a calculated mode at 1075 cm^{-1} in which essentially the same coupled vibrations occur but with the pyridyl 18b displacements having the opposite phase.

L Ligand Bands of 3. There are significant differences between the IR spectra of the electron-donor systems **1** and **2** and that of **3**, in which a terminal electron-donor substituent is absent, as shown by the spectra of **1** and **3** given together in Figure 2. The differences may be attributed to the absence of bands arising directly from the absent substituents, to weaker bands arising from smaller dipole changes during vibrations along the long axis of the L ligand of **3**,[44] or to band shifts arising from changes in bonding or the forms of mixed modes. The most notable absence in the spectrum of **3** is the band at 1395 cm^{-1} from **1** (and at 1374 cm^{-1} from **2**), consistent with its assignment to a mode involving a strong contribution from a ph−N stretching vibration that cannot occur in **3**. The bands at ca. 1618, 1604, 1512, 1487, and 1198 cm^{-1} are much weaker from **3** than from **1** and **2**, consistent with their assignment to modes involving 8a, 9a, 18a, and 19a vibrations that occur along the donor−acceptor axes of the phenyl and pyridyl groups and that may be expected to give smaller dipole changes due to the absence of the phenyl electron-donor substituent in **3**. The amide I band of **1** and **2** shifts up by ca. 13 cm^{-1} to occur at 1696 cm^{-1} for **3**, and this shift can be rationalized by an increase in CO bond strength due to a decreased contribution from the charge-transfer canonical form A in Scheme 3. There are also small upshifts of 3 and 1 cm^{-1} in bands assigned to modes involving pyridyl 8b/3 and 3 vibrations that occur at 1586 and 1333 cm^{-1}, respectively, in **3**.

L Ligand Bands of 4. There are significant differences between the IR spectra of **1** and **2** and that of **4**, in which a phenyl electron-donor substituent is present but in which the CH_2 spacer may be expected to increase the nonplanarity at the amide link and thereby decrease the electronic and vibrational coupling between the pyridyl ring and the other groups within the L ligand. The differences in the spectra may be attributed to the presence of additional bands arising directly from the CH_2 group, to weaker bands arising from smaller dipole changes during vibrations along the long axis of the L ligand because of weaker interactions between the phenyl and pyridyl rings in **4**,[44] or to band shifts arising from changes in bonding or the forms of the modes. The most notable change is that the amide I band of **2** shifts down by 28 cm^{-1} to occur at 1654 cm^{-1} for **4**, indicating a decrease in CO bond strength that can be rationalized by charge transfer from the NMe_2 group being more localized on the amide group because it is transmitted less effectively through to the pyridyl ring (Scheme 3; form B contributes less). The relatively large downshift of this band on introducing an insulator CH_2 group indicates that the electronic communication between the phenyl and the pyridyl rings of the L ligand is quite strong when it is absent, despite the small twist at the amide link, which is consistent with the other evidence from electronic and vibrational spectroscopy and also from the excited-state electron-transfer kinetics of **1** and **4**.[1] There are relatively small shifts in many of the other bands of the L ligand, as may be expected, and several are slightly weaker for **4** than for **2**, particularly those involving motion along the donor−acceptor axes of the phenyl and pyridyl groups. It is also notable that the band at 1374 cm^{-1} from **2**, assigned to a mode involving a strong contribution from ph−N stretching, is present as a moderately strong band at 1369 cm^{-1} in **4**, consistent with this assignment and with weaker charge transfer from the NMe_2 group due to weaker electron demand from the insulated Re−pyridyl group.

Ground-State IR Spectrum of 1-H^+. The addition of HCl to **1** in dichloromethane protonates the azacrown nitrogen atom to generate **1**-H^+, as determined by a strong blue-shift of the intraligand charge-transfer (ILCT) UV−vis absorption band;[1,2,8] the electron-donor character of the azacrown is removed as the nitrogen atom protonates to become fully pyramidal and sp^3 hybridized. The changes in the IR fingerprint region on protonation of **1** to give **1**-H^+ are significant, as shown in Figure 2, and they are similar in nature but generally larger in magnitude than those observed between the spectrum of **1** and the spectrum of **3**; they may be attributed, similarly, to weaker bands arising from smaller dipole changes[44] or to band shifts arising from changes in structure and bonding.

The 1395 cm^{-1} IR band of **1**, assigned to a mode involving ph−N stretching, is lost upon protonation, but a new band cannot be seen clearly, possibly being obscured by solvent or other sample bands. This band is well-established to be diagnostic of electronic structure in dialkylamino systems;[32,37,39,40,45−48] for example, a band of dimethylaniline at 1348 cm^{-1} is reported to shift down to 1245 cm^{-1} upon protonation,[37] consistent with the change to a ph−N single bond and an sp^3-hybridized nitrogen atom. The observation here is consistent with the changes we have reported for the alkene and alkyne analogues, where a band at ca. 1395 cm^{-1}, assigned to this mode, was strongly downshifted upon cation binding to the azacrown.[7]

The bands of **1** at 1618, 1604, 1512, 1487, and 1198 cm^{-1} assigned to modes involving 8a, 9a, 18a, and 19a vibrations lose intensity upon protonation, consistent with the loss of charge-transfer character. The amide I band of **1** shifts up by 13 cm^{-1} to 1696 cm^{-1} for **1**-H^+, as also observed on going from **1** to **3**, and this can be rationalized similarly by an increase in the amide CO bond strength due to a decreased contribution from the charge-transfer canonical form A in Scheme 3. The coupled amide II and pyridyl 18a/19a band of **1** shifts up slightly by 2 cm^{-1} to 1514 cm^{-1} for **1**-H^+, consistent with its position

at higher wavenumbers for amides that are not attached to an electron donor;[49,50] this mode has substantial ν(C−N) character, and its shift may be rationalized by an increase in the amide C−N bond strength due to an increased contribution from canonical form C in Scheme 3. There are also upshifts of 10 and 3 cm^{-1} in the bands assigned to modes involving pyridyl 8b/3 vibrations, which gave smaller shifts on going from **1** to **3** and which occur at 1593 and 1335 cm^{-1}, respectively, in **1**-H^+.

Ground-State IR Spectrum of 1-Ba^{2+}. The addition of barium perchlorate to **1** in acetonitrile results in metal cation complexation to the azacrown to generate **1**-Ba^{2+}, as determined by a moderately strong blue-shift of the ILCT UV−vis absorption band that is approximately half that observed upon protonation;[1,2,8] the electron-donor character of the azacrown is lowered by Ba^{2+} complexation. The IR spectrum of **1**-Ba^{2+} in acetonitrile shows $\nu(CO)_{Re}$ and bpy bands that are essentially identical to those of **1** (Figure 4 and Table 1),[51] indicating that Ba^{2+} complexation does not affect the Re center significantly in the ground state, whereas the L ligand bands of **1** show significant changes upon Ba^{2+} complexation (Figure 4) that are similar to those observed upon protonation (Figure 2) but smaller in magnitude.

The 1397 cm^{-1} band of **1** in CD_3CN, assigned to a mode involving ph−N stretching, loses all intensity, and the equivalent mode in **1**-Ba^{2+} is tentatively assigned to be a contributor to the broad feature that includes peaks at 1299 and 1275 cm^{-1}, consistent with our assignment of IR bands at 1250 cm^{-1} to this mode for the Ba^{2+}-complexed alkene and alkyne analogues.[7] The bands of **1** in CD_3CN at 1618, 1604, 1493, 1273, and 1200 cm^{-1} assigned to modes involving 8a, 9a, 18a, 19a, and ν(ph−N) vibrations become weaker, the amide I band shows a moderate upshift of 4 cm^{-1} to 1685 cm^{-1} in **1**-Ba^{2+}, and the bands assigned to modes involving pyridyl 8b/3 and 3 vibrations show small upshifts of 5 and 3 cm^{-1} to occur at 1593 and 1335 cm^{-1}, respectively, in **1**-Ba^{2+} (all in relation to their positions for **1** in CD_3CN). All of these effects are rationalized in the same way as those observed upon protonation, and the generally smaller magnitudes of the changes are attributed to an interaction with the azacrown N atom that is weaker for Ba^{2+} than for H^+.

Ba^{2+} Binding to the Amide Carbonyl Group. An additional IR band at 1662 cm^{-1} was observed from **1**-Ba^{2+} at the high barium perchlorate concentration required to ensure that the proportion of **1** without Ba^{2+} bound to the azacrown was minimal. This additional band can be attributed to a downshifted amide I mode arising from Ba^{2+} binding not only to the azacrown but also to the amide carbonyl group of **1**, as we discuss in detail next.

In general, an amide I band shifts significantly with solvent or other intermolecular interactions at the carbonyl group, and a downshift is indicative of a weaker amide C═O bond. Chalcone-substituted ferrocenes in acetonitrile have been shown to give a downshifted ν(CO) IR band due to Ca^{2+} interacting with a carbonyl group at very high Ca^{2+} concentration (ca. 0.1 mol dm^{-3}); and, in the case of a chalcone substituent with both azacrown and carbonyl groups, the addition of Ca^{2+} was reported first to give an upshifted band due to binding to the azacrown and then to give a downshifted band due to binding also to the carbonyl group at very high Ca^{2+} concentrations.[52] Our observations indicate that a comparable situation occurs for **1**, for which the 1685 cm^{-1} band is attributable to an upshifted amide I mode due to Ba^{2+} binding only to the azacrown, as discussed for protonation at the azacrown, and the 1662 cm^{-1} band is attributable to a downshifted amide I mode attributable to an additional amide C═O···Ba^{2+} interaction at very high Ba^{2+} concentrations.[53]

This effect was confirmed by the addition of Ba^{2+} to **2** in CD_3CN, as shown in Figure 5. The absence of an upshifted amide I band is consistent with the absence of an azacrown within **2**, and the growth of a downshifted amide I band at 1657 cm^{-1} may be attributed to Ba^{2+} binding to the amide carbonyl group at $[Ba^{2+}] \geq 0.4$ mol dm^{-3}, with an estimated very low binding constant of ca. 2 dm^3 mol^{-1}. The only other significant change in the IR spectrum of **2** at high Ba^{2+} concentrations is a ca. 7 cm^{-1} upshift of the band at 1276 to 1283 cm^{-1}, which is consistent with its assignment to an amide III mode involving CN stretching (Figure 5 and Table 1) and to an increased contribution from canonical form C (Scheme 3) giving a stronger C−N bond on Ba^{2+} binding to the amide carbonyl. Both the positions and the intensities of the other IR bands are remarkably unaffected, with the only other changes being a slight broadening of the ca. 1605 and 1332 cm^{-1} bands to lower and higher wavenumbers, respectively. The absence of other changes indicates that the effect of Ba^{2+}−carbonyl binding is essentially localized at the amide group, and thus, it appears to be similar to a carbonyl solvation effect. This limited effect of Ba^{2+} on the IR bands of **2** contrasts its much more substantial effect on the IR band positions and intensities of **1**, for which the changes are therefore attributable predominantly to Ba^{2+} binding to the azacrown inducing changes throughout the L ligand, as discussed previously.

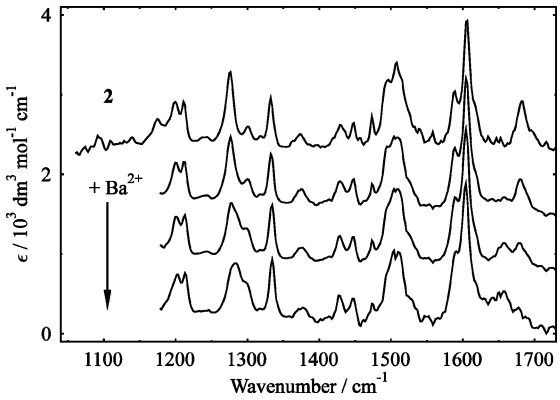

Figure 5. Fingerprint-region IR spectra of **2** in CD_3CN, in the absence and presence of barium perchlorate at 0.19, 0.46, and 0.73 mol dm^{-3} (region of strong perchlorate absorption omitted, and spectra offset for clarity).

The IR and TRIR studies of **1**-Ba^{2+} we report here were carried out on samples in which the presence of **1** without Ba^{2+} bound to the azacrown was minimized to ≤2% to ensure that the TRIR bands could be attributed unambiguously to excitation of **1**-Ba^{2+}, with Ba^{2+} bound to the azacrown, and not to the excitation of **1**. This strategy dictated the use of high ionic strengths and very high Ba^{2+} concentrations (≥0.5 mol dm^{-3}), which were typically at ≥50-fold in excess of the already high concentrations of **1** (≤10^{-2} mol dm^{-3}) that were needed due to a combination of low sample IR absorption coefficients and a short path length (100 μm) required because of strong solvent absorption. From the binding constants of ca. 126 and 2 dm^3 mol^{-1} for Ba^{2+} attaching to the azacrown[2] and amide carbonyl groups, respectively, these conditions gave samples comprising almost entirely **1**-Ba^{2+}, with Ba^{2+} bound to the azacrown, but with the azacrown-and-amide-bound form also present (typically ca. 35:65).[54] Earlier TRVIS[2] and emission[8] studies that established the general photochemical mechanisms of **1**-M^{n+} were carried out on samples with **1** at much lower concentrations of ca. 10^{-4} to 10^{-5} mol dm^{-3}, due to the higher sensitivity of these techniques, and generally at lower ionic strengths and M^{n+} concentrations at which binding to the amide carbonyl would generally not be significant. Our photochemical studies under conditions where M^{n+} binding to the amide carbonyl of **1** occurs

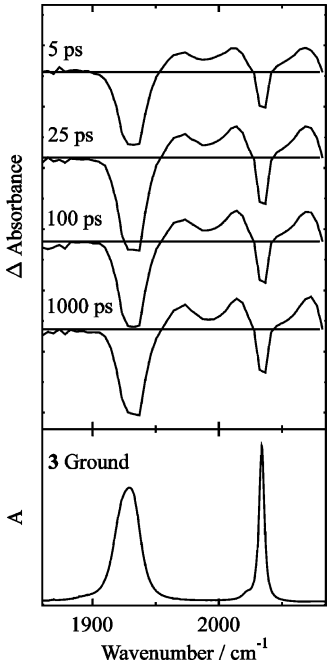

Figure 6. ν(CO)-region IR spectrum of **3** along with TRIR spectra recorded upon 400 nm excitation, all in CH_3CN.

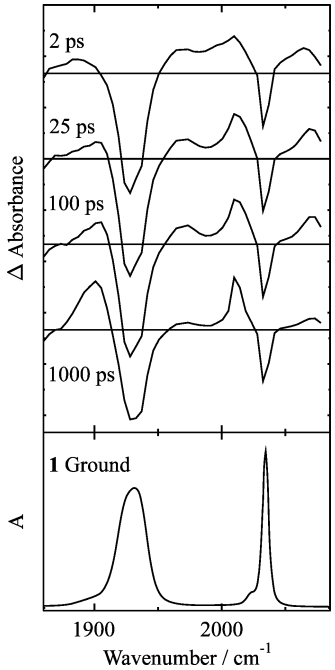

Figure 7. ν(CO)-region IR spectrum of **1** along with TRIR spectra recorded upon 400 nm excitation, all in CH_3CN.

to some extent, both here and in our earlier Raman work,[3] have not shown any effects that we can attribute to it having a strong influence on the overall photochemistry, with the only clear effect that we have observed being on the excited-state amide I IR band position. Hence, our observations suggest that an amide-bound metal cation may act principally as a spectator in the photochemistry of **1**-M^{n+}; however, they indicate that the effect should be considered carefully in designing and studying metal cation sensors and switches containing both azacrown and carbonyl groups, as noted also in a recent report on azacrown-substituted chromenes.[55]

Excited-State TRIR Spectra of 1 and 3. The Re → bpy MLCT transition in these [(bpy)Re(CO)$_3$L]$^+$ complexes gives a broad UV−vis absorption band peaking at ca. 350 nm that is distinct for **3** and that is responsible for the absorption tail at >390 nm, which emerges from under the strong ILCT band of **1** that dominates at shorter wavelengths.[1,2,8] The TRIR spectra reported here were recorded upon pumping at 400 nm, which populates the Re → bpy MLCT excited states of **1** and **3**.[1] Table 1 gives band positions and possible assignments of the excited-state bands that are discussed in detail next.

ν(CO) Region. The TRIR spectrum of **3** in the ν(CO) region (Figure 6) consists of bleaches of the ground-state bands at 2035 and 1931 cm^{-1} and three transient bands at higher wavenumbers that persist for ≥2 ns, after showing narrowing and a small upshift in wavenumber over the first ca. 15 ps that are consistent with vibrational relaxation in the excited state.[15−19,22,56] These transient bands at 2073, 2014, and 1973 cm^{-1} (Table 1) are upshifted from the ground-state positions by ca. 38, 83, and 42 cm^{-1}, respectively, and they are characteristic of the MLCT excited state of a (bpy)Re(CO)$_3$L complex in which oxidation to Re^{II} (Scheme 1) results in weaker backbonding to the CO ligands.[9−22] The observation of three $\nu(CO)_{Re}$ bands from the MLCT state is attributable to a lowering of the pseudo-C_{3v} symmetry that resulted in the observation of only two $\nu(CO)_{Re}$ bands in the ground state.

The TRIR spectrum of **1** at early times of ca. <100 ps (Figure 7) is very similar to that of **3**, comprising bands at 2069, 2010, and 1973 cm^{-1} at 25 ps, and hence, it is readily assigned to the

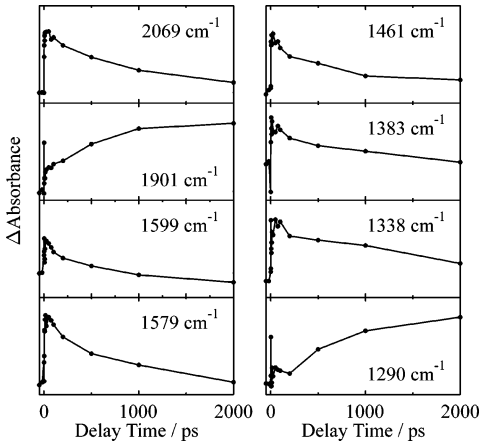

Figure 8. TRIR kinetic traces recorded upon 400 nm excitation of **1**; ν(CO) region in CH_3CN, fingerprint region in CD_3CN.

MLCT excited state of **1** (Table 1). In contrast to that of **3**, the TRIR spectrum of **1** evolves at later times, with the MLCT-state bands decaying and new bands at lower wavenumbers than the ground-state bands growing in to give peaks at 2010 and 1901 cm^{-1} at ≥1 ns. The TRIR kinetics essentially match those that we observed by TRVIS,[57] as illustrated in Figure 8 by the concomitant decay and growth of the bands at 2069 and 1901 cm^{-1}, respectively, and so the TRIR spectrum at late times (≥1 ns) is assigned to the LLCT state of **1** (Scheme 1).[1] The bands at 2010 and 1901 cm^{-1} support this assignment because their downshifts of 25 and 29 cm^{-1} from the respective ground-state positions indicate that the CO bonds are weaker, consistent with stronger backbonding from a Re^{I} center that is attached to a bpy$^{\bullet-}$ ligand in the LLCT state; the return to a two-band pattern indicates a return to pseudo-C_{3v} symmetry in going from MLCT to LLCT states. Similar ν(CO) band positions and downshifts have been reported upon electrochemical reduction of (bpy)Re(CO)$_3$Cl to form [(bpy$^{\bullet-}$)Re(CO)$_3$Cl][12] and upon photochemical formation of similar LLCT states of Re(CO)$_3$ systems with quite different diimine and L ligands.[19,21] The

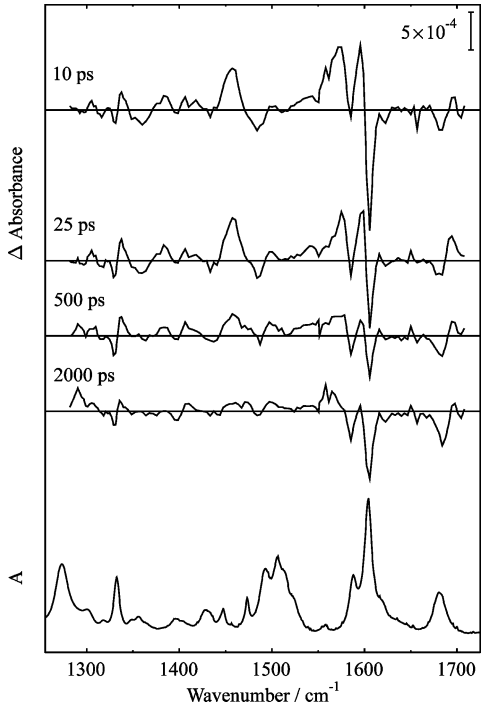

Figure 9. Fingerprint-region IR spectrum of **1** along with TRIR spectra recorded upon 400 nm excitation, all in CD_3CN.

TRIR spectrum of **1** in the LLCT state we report here is consistent with our nanosecond transient resonance Raman studies,[3] where we observed one resonance-enhanced Raman $\nu(CO)_{Re}$ band at 2012 cm^{-1} that matches the high-wavenumber TRIR band observed here.

Fingerprint Region. The TRIR spectra of **1** in the fingerprint region (Figure 9) show bleaches of many of the ground-state bands and several new excited-state bands. Following small upshifts and narrowing at <25 ps attributable to vibrational relaxation, the spectra at early times (≤200 ps) show strong and distinct excited-state peaks at ca. 1694, 1599, 1579, 1461, 1383, and 1338 cm^{-1} that can be assigned to the MLCT state. These bands show decay kinetics on a time scale that matches the TRIR decay kinetics of the $\nu(CO)_{Re}$ bands of the MLCT state (Figures 8 and 9), supporting this assignment. The spectra at early times also show weaker or less distinct features at ca. 1616, 1558, 1544, 1497, 1406, and 1308 cm^{-1} that also may arise from the MLCT state, although their decay kinetics are less clear.

The TRIR band at 1694 cm^{-1} is assigned to the amide I mode in the MLCT state (Table 1), upshifted by 13 cm^{-1} from its ground-state position at 1681 cm^{-1} in CD_3CN. The assignment of the other MLCT-state bands is less straightforward, but some tentative assignments can be proposed. The TRIR peaks at 1616 (weak), 1599, and 1579 cm^{-1} are tentatively assigned to ca. 2, 5, and 9 cm^{-1} downshifted counterparts of the three ground-state bands at 1618, 1604, and 1588 cm^{-1}, respectively (in CD_3CN), which were assigned to modes involving phenyl 8a/9a, pyridyl 8a/9a, and NH bend coupled to pyridyl 8b/3 vibrations (Table 1).[58] The sloping feature at slightly lower wavenumbers may include peaks at ca. 1558 and 1544 cm^{-1} or may arise as the shoulder of broad bands giving strong peaks at ca. 1599 and 1579 cm^{-1}. The TRIR bands at 1497 and 1461 cm^{-1}, which occur at either side of a bleaching peak at ca. 1484 cm^{-1}, are tentatively assigned to ca. 17 and 32 cm^{-1} downshifts of the ground-state bands at 1514 and 1493 cm^{-1}, respectively (in CD_3CN), that were assigned to modes involving coupled amide II and pyridyl 18a vibrations. These modes were calculated to be strongly mixed in the ground state, and their forms may change significantly in the excited state; the ground-state spectrum gives several bands in this region that are notably sensitive to solvent, as can be seen by comparing Figures 1 and 4. The broad TRIR feature with peaks at ca. 1406 and 1383 cm^{-1} includes a minimum due to bleaching of the ground-state band at 1397 cm^{-1}, which was assigned to a mode involving ph−N stretching. The TRIR band at 1406 cm^{-1} is tentatively assigned to a 22 cm^{-1} downshift of the ground-state band assigned to a pyridyl 18b/14 vibration and that at 1383 cm^{-1} to a 14 cm^{-1} downshift of the ground-state band assigned to the mode involving ν(ph−N) and 18a/19a phenyl vibrations. The TRIR bands at 1338 and 1308 cm^{-1} are assigned to ca. 6 and 7 cm^{-1} upshifts of the ground-state bands at 1332 and 1301 cm^{-1}, which were assigned to pyridyl and phenyl 3 modes, respectively. Our assignment of all these fingerprint TRIR bands to L ligand rather than bpy modes is consistent with the reported TRIR spectra of $[Ru(bpy)_3]^{2+}$ and a related $[Re(bpy)(CO)_3L]^+$ system,[31] which show that the MLCT-state $bpy^{\bullet-}$ bands are much weaker than the ground-state bpy bleaching bands, which are very weak in the TRIR spectra observed here. By contrast, the transient resonance Raman spectra that we have reported gave strong $bpy^{\bullet-}$ bands of **1** in the MLCT and LLCT states.[3]

Although MLCT excitation is localized at the $(bpy)Re(CO)_3$ group, the TRIR bands in the fingerprint region indicate clearly that it responds also in significant changes within the L ligand. The 13 cm^{-1} upshift of the amide I band indicates that the amide CO bond becomes stronger in the MLCT state, and this is attributable to increased electron demand from the Re^{II} center withdrawing electron density from the amide carbonyl group, such that donation from the phenyl−azacrown is transmitted more effectively through to the pyridyl group (Scheme 3; form B contributes more and C less). The ca. 17 and 32 cm^{-1} downshifts of two bands assigned to amide II modes, which involve amide C−N stretching, may be attributed to the same effect, with the withdrawal of electron density weakening the amide C−N bond and strengthening the py−N bond in the MLCT state (Scheme 3; form B contributes more and C less); these shifts may arise also, in part, from a change in the form of the modes, and particularly those involving the amide II vibration, which gives two bands from strongly mixed modes in the ground state. The downshift of the phenyl and pyridyl 8a/9a modes may be attributed to the pyridyl and phenyl rings adopting a more quinoidal structure[38,39] as a result of increased charge-transfer character due to the greater electron demand by the Re^{II} center in the MLCT state (Scheme 3; canonical forms B and A, respectively, contribute more); the observation of features at lower wavenumbers than the ground-state bands at ca. 1600 cm^{-1}, along with the absence of any at higher wavenumbers, supports this interpretation regardless of the precise excited-state band positions and mode assignments.

This interpretation is supported by the observation that some of the band shifts on going from the ground state to the MLCT state of **1** are in the opposite direction to those observed on going from **1** to **4** in the ground state. The TRIR spectrum of **1** shows an upshift of the amide I band in going to the MLCT state, attributed to excitation increasing the extent of electron transfer to the Re center, whereas it shifts down upon going from **1** to **4**, attributed to the CH_2 insulator decreasing the extent of electron transfer to the Re center. The three bands at ca. 1600 cm^{-1} assigned to phenyl 8a/9a, pyridyl 8a/9a, and coupled NH bending and 8b/3 pyridyl modes show downshifts in going to the MLCT state of **1**, attributed to increased quinoidal character

due to increased charge-transfer character, whereas they shift up upon going to **4**, attributed to decreased charge-transfer character.

Several TRIR bands in the fingerprint region show similar decay kinetics to those recorded in the ν(CO) region (Figures 7−9), consistent with the decay of the MLCT state, and the fingerprint-region spectrum of **1** at ≥1 ns (Figure 9) can be assigned similarly to the LLCT state. This TRIR spectrum shows the same bleaching of ground-state bands observed at earlier times, but the fingerprint-region bands of the LLCT state are notably much weaker than those of the MLCT state, contrasting the similar strengths of the transient bands from these states in the ν(CO) region (Figure 7). Only one new TRIR band, a weak feature at 1290 cm^{-1} (Figure 9), is observed unambiguously from the kinetics (Figure 8) to grow in on the same time scale as the formation of the LLCT state. Some small band shifts are observed on the same time scale (Figure 9): the amide I band at 1694 cm^{-1}, the 8a/9a phenyl band at 1596 cm^{-1}, and the NH bend band at 1575 cm^{-1} all appear to shift slightly to higher wavenumbers as the strong, overlying MLCT excited-state bands decay; however, these bands are weak at later times, they overlap with strong ground-state bleaches that may distort their profiles, and so these possible assignments are uncertain.

Although the TRIR spectrum of the LLCT state of **1** is sparse, it provides some structural information. The one new band at 1290 cm^{-1} that can be attributed unambiguously to the LLCT state may tentatively be assigned to a mode involving ph−N stretching, downshifted by ca. 107 cm^{-1} from a band at 1397 cm^{-1} in the ground state and by ca. 93 cm^{-1} from a possible equivalent band at 1383 cm^{-1} in the MLCT state. It is reasonable to propose that the TRIR difference spectrum will show bands of the phenyl group, where the changes in the L ligand are most significant between ground and LLCT states, and our tentative assignment is based on studies reported for DMABN and its isotopomers,[32,47,48] for which the strongest (although weak) band at 1276 cm^{-1} in the TRIR spectrum of the CT state has been assigned to a mode involving ph−N stretching, shifted down by 96 cm^{-1} from a ground-state band at 1372 cm^{-1}. We observed only one strong LLCT-state band in the time-resolved resonance Raman spectrum in this region,[3] which was a dominant feature at 1514 cm^{-1} that we assigned to a ca. 100 cm^{-1} downshift of the phenyl 8a/9a band from its ground-state position; it is not observed in the TRIR spectrum here, consistent with the equivalent ground-state IR band being relatively weak. The observation that the IR bands from the LLCT state are significantly weaker than the strong bands from the ground and MLCT states is indicative of smaller dipole changes upon vibration, which is consistent with the electron-donating properties of the azacrown nitrogen atom being lost due to its oxidation in forming the LLCT state and with the electron-acceptor properties of the rhenium center being lowered upon its reduction from Re^{II} back to Re^{I} in going from the MLCT state to the LLCT state (Scheme 1).

Excited-State TRIR Spectra of 1-Ba^{2+}. *ν(CO) Region.* The TRIR spectrum observed in the ν(CO) region upon excitation of **1**-Ba^{2+} (Figure 10) has a similar profile to that from **1** at early times (Figure 7) and that from **3** at all delay times (Figure 6), showing a set of three excited-state bands at higher wavenumbers than the ground-state bands; it may be assigned similarly to an MLCT state, with peaks at ca. 2069, 2011, and 1970 cm^{-1} observed at 25 ps after upshifts and narrowing at early times. Whereas the TRIR spectrum from **1** shows large band shifts to lower wavenumber over ca. 1 ns as the LLCT state forms (Figure 7), the spectrum from **1**-Ba^{2+} (Figure 10) clearly does not show such shifts, indicating that the presence of Ba^{2+} extends the MLCT-state lifetime of **1**, consistent with the proposal that electron transfer to form the LLCT state is thermodynamically unfavorable when a metal cation is bound to the azacrown.[2,8] The persistence of the TRIR bands of the MLCT state indicates that Ba^{2+} remains bound to the azacrown for at least ca. 1 ns after excitation, consistent with a time scale of ca. 40 ns for its release to bulk solution (k_{off}^{-1}; Scheme 2) obtained by analyzing nanosecond TRVIS data[2] and supported by time-resolved resonance Raman data.[3]

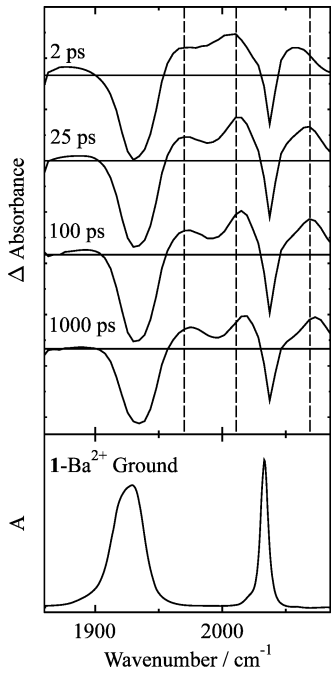

Figure 10. ν(CO)-region IR spectrum of **1**-Ba^{2+} along with TRIR spectra recorded upon 400 nm excitation, all in CH_3CN.[54] Dashed lines indicate the maxima at 25 ps.

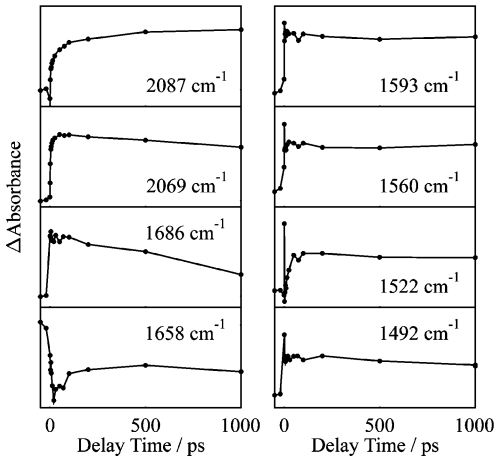

Figure 11. TRIR kinetic traces recorded upon 400 nm excitation of **1**-Ba^{2+}; ν(CO) region in CH_3CN and fingerprint region in CD_3CN.[54,60]

Although the profile of the TRIR spectrum from the MLCT state of **1**-Ba^{2+} persists, all three $\nu(CO)_{Re}$ bands show ca. 5−10 cm^{-1} upshifts between ca. 25 ps and 1−2 ns (Figure 10) to give peaks at 2073, 2020, and 1975 cm^{-1} at 1 ns, whereas the $\nu(CO)_{Re}$ bands of the MLCT state of **3** do not show such shifts on this time scale (Figure 6). The TRIR kinetic traces in Figure 11 illustrate this effect further, showing minor growth and decay in the signals at 2087 and 2069 cm^{-1}, respectively, as the upshift occurs. The possible origins of this effect are discussed next.

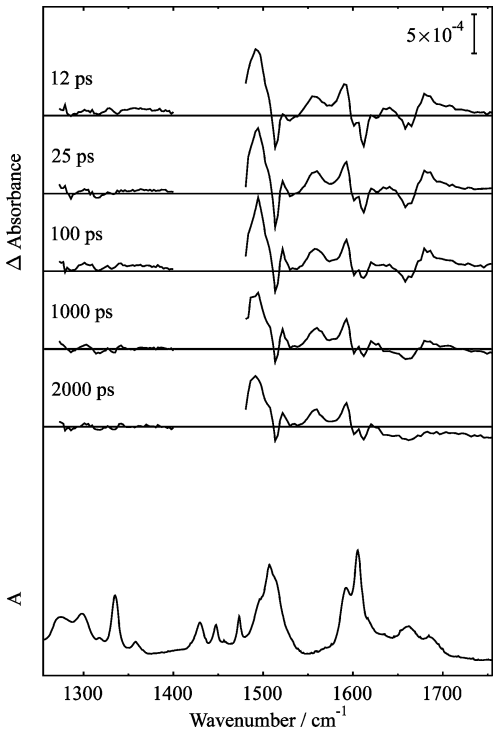

Figure 12. Fingerprint-region IR spectrum of **1**-Ba^{2+} along with TRIR spectra recorded upon 400 nm excitation, all in CD_3CN.[54,59]

Fingerprint Region. The fingerprint-region TRIR spectra observed upon excitation of **1**-Ba^{2+} (Figure 12)[59] show bleaches of ground-state bands and several new excited-state bands. Following small upshifts and narrowing at <50 ps, the spectra show strong and distinct excited-state peaks at ca. 1593, 1560, 1522, and 1492 cm^{-1} and weak features at ca. 1342 and 1303 cm^{-1}, which undergo almost no change up to ca. 2 ns, as shown also by the TRIR kinetics (Figure 11). These bands can be assigned to the MLCT state of **1**-Ba^{2+}.

The TRIR bands from **1**-Ba^{2+} in the MLCT state at 1593 and 1560 cm^{-1} are tentatively assigned to the ca. 12 and 33 cm^{-1} downshifted counterparts of the strong ground-state bands of **1**-Ba^{2+} at 1605 and 1593 cm^{-1}, respectively, which were assigned to modes involving pyridyl 8a/9a vibrations and NH bending coupled to pyridyl 8b/3 vibrations (Table 1). This assignment indicates that these pyridyl modes are more strongly downshifted in going from the ground to MLCT state of **1**-Ba^{2+} than they are in going from the ground to MLCT state of **1**, where they were tentatively assigned to respective bands at 1599 and 1579 cm^{-1}, downshifted by ca. 5 and 9 cm^{-1} from the ground-state counterparts in **1**, which overlapped strongly with the bleaching bands in the TRIR spectra (Figure 9).[58] The strong TRIR feature from **1**-Ba^{2+} at ca. 1480−1530 cm^{-1} comprises a strong broad peak at 1492 cm^{-1}, a bleaching peak at 1514 cm^{-1}, and a feature peaking at 1522 cm^{-1} that may arise as a shoulder of the strong band at lower wavenumber or as a distinct band; the overall pattern in this region resembles that of the strong TRIR feature from **1** at ca. 1440−1510 cm^{-1} (Figure 9), although the feature is ca. 30 cm^{-1} higher for **1**-Ba^{2+}. The strong TRIR band from the MLCT state of **1**-Ba^{2+} at 1492 cm^{-1} is tentatively assigned to a 15 cm^{-1} downshift of the ground-state band at ca. 1507 cm^{-1} assigned to coupled amide II and pyridyl 18a vibrations; as discussed previously, the bands in this region are sensitive to solvent for **1** (Figures 1 and 5), and they are assigned to mixed modes (Table 1) that may be expected to change significantly in the excited state. The very weak TRIR bands at 1342 and 1303 cm^{-1} from **1**-Ba^{2+} are tentatively assigned to ca. 7 and 4 cm^{-1} upshifts of the ground-state bands at 1335 and 1299 cm^{-1}, which were assigned to pyridyl and phenyl 3 modes, respectively, and which give a similar pattern to the slightly stronger TRIR bands observed in this region from **1**. Several of the TRIR bands from the MLCT state of **1**-Ba^{2+} (Figure 12) are weaker than the equivalent TRIR bands from the MLCT state of **1** (Figure 9): most notably the bands at 1593 and 1599 cm^{-1}, respectively, assigned to a pyridyl 8a/9a vibration. This observation is consistent with the occurrence of smaller dipole changes upon vibration due to weaker electron donation when Ba^{2+} is complexed to the azacrown, as observed and discussed for the equivalent ground-state spectra (Figure 4) and as indicated by several TRIR bleaching bands that are weaker for **1**-Ba^{2+} (Figure 12) than **1** (Figure 9).

Whereas the TRIR spectra from **1**-Ba^{2+} at ca. 1200−1640 cm^{-1} are essentially unchanged between ca. 50 ps and 2 ns, the TRIR bands assigned to amide I modes at ca. 1640−1750 cm^{-1} show significant changes over ca. 1−2 ns (Figure 12), with a time dependence (Figure 11)[60] that appears to match that of the small upshifts in the $\nu(CO)_{Re}$ TRIR bands discussed previously (Figures 10 and 11). The TRIR spectrum at early times shows a bleach of the ground-state amide I band at ca. 1662 cm^{-1}, assigned above to **1** with Ba^{2+} bound to both the azacrown and the amide carbonyl group, and an increase in absorption at ca. 1685 cm^{-1}, which corresponds to the ground-state amide I band assigned to **1** with Ba^{2+} bound only to the azacrown. These bleaching and new absorption bands decay to give a TRIR spectrum at ca. 2 ns that is essentially featureless in this region (apart from baseline drift), indicating that the amide I band position in the MLCT state present at this time is similar to that of the ground state. Hence, the TRIR data seem to suggest that excitation to the MLCT state results in rapid disruption of C═O···Ba^{2+} interactions at the amide carbonyl group, which then recover in ca. 1−2 ns, and that the amide I band position in the MLCT state is little changed from that in the ground state once this interaction is restored. As discussed, the $\nu(CO)_{Re}$ TRIR bands show a small upshift in ca. 1−2 ns that indicates a decrease in electron density at the Re center, which is consistent with a shift in electron density toward the L ligand that might be caused by the restoration of a Ba^{2+} interaction with the amide carbonyl. The absence of large changes in any of the other TRIR bands in ca. 1−2 ns also may be consistent with this interpretation because the introduction of the C═O···Ba^{2+} interaction results in relatively little changes in the other bands in the ground-state IR spectrum of **2** (Figure 5). Another possibility is that the changes on this time scale may arise also from changes in the nature of the Ba^{2+} interaction with the azacrown, as has been discussed in interpreting picosecond TRVIS data observed upon excitation of M^{n+}-bound organic−azacrown systems.[61−65] However, the TRIR spectrum can be attributed to the MLCT state of **1**-Ba^{2+}, regardless of the precise origin of the relatively subtle changes over ca. 1−2 ns, and it is clearly different from that of the MLCT state of **1** when Ba^{2+} is not bound to the azacrown.

The similarities and differences between the fingerprint-region TRIR spectra of the MLCT states of **1**-Ba^{2+} and **1** are notable. They show a similar set of excited-state bands and a net increase in absorbance from the ground state that are both attributable to a significant charge redistribution within the L ligand whether or not Ba^{2+} is bound to the azacrown and despite the MLCT excitation nominally being localized on the (bpy)$Re(CO)_3$ group. From the tentative assignments proposed here, it appears that at least some of the pyridyl bands show shifts that are larger upon MLCT excitation of **1**-Ba^{2+} than **1**, whereas at least some

of the amide and phenyl bands show smaller shifts. These differences in the shift patterns suggest that the increased electron demand of the Re^{II} center in the MLCT state results in charge redistribution that is relatively localized at the pyridyl ring for **1**-Ba^{2+} and more delocalized for **1**, and this effect may reasonably be attributed to the electron-donor properties of the phenyl−azacrown group being lowered when Ba^{2+} is bound to the azacrown.

Conclusion

We have reported ground- and excited-state IR spectra of **1**, its model complexes, and its protonated and Ba^{2+}-complexed forms. These IR spectra have been shown to provide not only characteristically strong CO stretching bands from the $(bpy)Re(CO)_3$ group but also a rich set of bands in the fingerprint region that provide useful information on structure and bonding within the L ligand.

The ground-state IR spectrum of **1** is dominated in the fingerprint region by bands arising principally from L ligand pyridyl and amide vibrations, and their assignments are consistent with our earlier RR assignments,[3] for which they provide further support. The TRIR spectra of **1** give $\nu(CO)_{Re}$ marker bands that characterize the MLCT and LLCT states conclusively, with their positions supporting the assignments made earlier by nanosecond transient Raman spectroscopy[3] and their time dependence supporting the time scale for intramolecular electron transfer to form the LLCT state determined earlier by picosecond time-resolved UV−vis spectroscopy.[1] Importantly, the fingerprint-region TRIR spectra of **1** also provide completely new information. The MLCT state gives strong L ligand TRIR bands, with most tentatively assigned to pyridyl and amide vibrations, which indicate that the increased electron demand at the Re^{II} center results in significant charge redistribution within the L ligand. By contrast, the LLCT state gives a sparse TRIR spectrum, which indicates that the return to a Re^{I} center largely restores the charge distribution of the ground state at the pyridyl group, with one weak L ligand band being assigned tentatively to a mode of the oxidized phenyl−azacrown group.

Upon addition of Ba^{2+}, the ground-state IR spectrum of **1** shows several expected band shifts that we attribute to Ba^{2+} binding to the azacrown; some other changes, principally in the amide I band position, we attribute to Ba^{2+} binding also to the amide carbonyl group at the high concentrations required for TRIR studies. The TRIR spectra of **1**-Ba^{2+} give $\nu(CO)_{Re}$ marker bands that characterize the MLCT state of **1**-Ba^{2+} conclusively, with their positions supporting the assignments made earlier by nanosecond transient Raman spectroscopy[3] and their persistence over ca. 2 ns supporting the time scale of ca. 40 ns for Ba^{2+} release determined earlier by nanosecond time-resolved UV−vis[2] and resonance Raman[3] spectroscopy. The fingerprint-region TRIR spectra again provide new information, giving strong L ligand bands from **1**-Ba^{2+} in the MLCT state that are similar to those from **1** but shifted in position, indicating that the increased electron demand at the Re^{II} center still results in significant charge redistribution within the L ligand even when Ba^{2+} is bound to the azacrown. This direct evidence from TRIR spectroscopy that MLCT excitation of **1**-Ba^{2+} significantly affects the electronic structure of the L ligand as well as the $(bpy)Re(CO)_3$ group is an important observation because it supports the proposal that charge redistribution within the L ligand in the MLCT state is sufficiently strong to lower the binding constant and drive the general mechanism for light-controlled release of a metal cation from the azacrown in this class of complexes.

The use of time-resolved infrared spectroscopy has been shown to be particularly useful in this study because it has provided vibrational information that was not available from time-resolved UV−visible absorption or emission spectroscopy,[1,2] and L ligand bands that complement the $(bpy)Re(CO)_3$ bands that were the principal features of the transient resonance Raman spectra.[3] Overall, though, it is the combination of the results from all four of these time-resolved techniques that has enabled the generic light-controlled ion-switching mechanism to be elucidated.

This study also illustrates a general effect in transition-metal photochemistry that can be deployed in designing supramolecular switches: MLCT excitation that is nominally localized on one ligand, which is reduced upon excitation, results in an oxidized metal center whose increased electron demand induces significant charge redistribution that is sufficient to induce a reaction at a relatively remote site within another attached ligand. In the example studied here, Re → bpy MLCT excitation induces significant charge redistribution that results ultimately in ion release from a pyridyl−amido−phenyl−azacrown ligand that is not fully conjugated and in which the azacrown lies at >10 Å from the Re center.[66]

Acknowledgment. We thank L. C. Abbott, P. Matousek, and A. W. Parker for assistance and helpful discussions and the EPSRC for financial support.

References and Notes

(1) Lewis, J. D.; Bussotti, L.; Foggi, P.; Perutz, R. N.; Moore, J. N. *J. Phys. Chem. A* **2002**, *106*, 12202.
(2) Lewis, J. D.; Perutz, R. N.; Moore, J. N. *J. Phys. Chem. A* **2004**, *108*, 9037.
(3) Lewis, J. D.; Clark, I. P.; Moore, J. N. *J. Phys. Chem. A* **2007**, *111*, 50.
(4) Lewis, J. D.; Perutz, R. N.; Moore, J. N. *Chem. Commun. (Cambridge, U.K.)* **2000**, 1865.
(5) Lewis, J. D.; Moore, J. N. *Chem. Commun. (Cambridge, U.K.)* **2003**, 2858.
(6) Lewis, J. D.; Moore, J. N. *Dalton Trans.* **2004**, 1376.
(7) Lewis, J. D.; Moore, J. N. *Phys. Chem. Chem. Phys.* **2004**, *6*, 4595.
(8) MacQueen, D. B.; Schanze, K. S. *J. Am. Chem. Soc.* **1991**, *113*, 6108.
(9) Schoonover, J. R.; Bignozzi, C. A.; Meyer, T. J. *Coord. Chem. Rev.* **1997**, *165*, 239.
(10) Schoonover, J. R.; Strouse, G. F. *Chem. Rev.* **1998**, *98*, 1335.
(11) Butler, J. M.; George, M. W.; Schoonover, J. R.; Dattelbaum, D. M.; Meyer, T. J. *Coord. Chem. Rev.* **2007**, *251*, 492.
(12) George, M. W.; Johnson, F. P. A.; Westwell, J. R.; Hodges, P. M.; Turner, J. J. *J. Chem. Soc., Dalton Trans.* **1993**, 2977.
(13) Gamelin, D. R.; George, M. W.; Glyn, P.; Grevels, F.-W.; Johnson, F. P. A.; Klotzbucher, W.; Morrison, S. L.; Russell, G.; Schaffner, K.; Turner, J. J. *Inorg. Chem.* **1994**, *33*, 3246.
(14) Schoonover, J. R.; Strouse, G. F.; Dyer, R. B.; Bates, W. D.; Chen, P.; Meyer, T. J. *Inorg. Chem.* **1996**, *35*, 273.
(15) Abbott, L. C.; Arnold, C. J.; Ye, T.-Q.; Gordon, K. C.; Perutz, R. N.; Hester, R. E.; Moore, J. N. *J. Phys. Chem. A* **1998**, *102*, 1252.
(16) Towrie, M.; Grills, D. C.; Dyer, J.; Weinstein, J. A.; Matousek, P.; Barton, R.; Bailey, P. D.; Subramaniam, N.; Kwok, W. M.; Ma, C.; Phillips, D.; Parker, A. W.; George, M. W. *Appl. Spectrosc.* **2003**, *57*, 367.
(17) Dyer, J.; Blau, W. J.; Coates, C. G.; Creely, C. M.; Gavey, J. D.; George, M. W.; Grills, D. C.; Hudson, S.; Kelly, J. M.; Matousek, P.; McGarvey, J. J.; McMaster, J.; Parker, A. W.; Towrie, M.; Weinstein, J. A. *Photochem. Photobiol. Sci.* **2003**, *2*, 542.
(18) Liard, D.; Busby, M.; Farrell, I. R.; Matousek, P.; Towrie, M.; Vlček, A., Jr. *J. Phys. Chem. A* **2004**, *108*, 556.
(19) Busby, M.; Gabrielsson, A.; Matousek, P.; Towrie, M.; Di Bilio, A. J.; Gray, H. B.; Vlček, A., Jr. *Inorg. Chem.* **2004**, *43*, 4994.
(20) Dattelbaum, D. M.; Martin, R. L.; Schoonover, J. R.; Meyer, T. J. *J. Phys. Chem. A* **2004**, *108*, 3518.
(21) Gabrielsson, A.; Hartl, F.; Zhang, H.; Lindsay Smith, J. R.; Towrie, M.; Vlček, A., Jr.; Perutz, R. N. *J. Am. Chem. Soc.* **2006**, *128*, 4253.
(22) Gabrielsson, A.; Busby, M.; Matousek, P.; Towrie, M.; Hevia, E.; Cuesta, L.; Perez, J.; Záliš, S.; Vlček, A., Jr. *Inorg. Chem.* **2006**, *45*, 9789.
(23) MacQueen, D. B.; Schanze, K. S. *J. Am. Chem. Soc.* **1991**, *113*, 7470.

(24) Frisch, M. J.; Trucks, G. W.; Schlegel, H. B.; Scuseria, G. E.; Robb, M. A.; Cheeseman, J. R.; Zakrzewski, V. G.; Montgomery, J. A., Jr.; Stratmann, R. E.; Burant, J. C.; Dapprich, S.; Millam, J. M.; Daniels, A. D.; Kudin, K. N.; Strain, M. C.; Farkas, O.; Tomasi, J.; Barone, V.; Cossi, M.; Cammi, R.; Mennucci, B.; Pomelli, C.; Adamo, C.; Clifford, S.; Ochterski, J.; Petersson, G. A.; Ayala, P. Y.; Cui, Q.; Morokuma, K.; Malick, D. K.; Rabuck, A. D.; Raghavachari, K.; Foresman, J. B.; Cioslowski, J.; Ortiz, J. V.; Baboul, A. G.; Stefanov, B. B.; Liu, G.; Liashenko, A.; Piskorz, P.; Komaromi, I.; Gomperts, R.; Martin, R. L.; Fox, D. J.; Keith, T.; Al-Laham, M. A.; Peng, C. Y.; Nanayakkara, A.; Gonzalez, C.; Challacombe, M.; Gill, P. M. W.; Johnson, B.; Chen, W.; Wong, M. W.; Andres, J. L.; Gonzalez, C.; Head-Gordon, M.; Replogle, E. S.; Pople, J. A. *Gaussian 98*, revision A.7; Gaussian, Inc.: Pittsburgh, PA, 1998.

(25) Flükiger, P.; Lüthi, H. P.; Portmann, S.; Weber, J. *MOLEKEL 4.0*; Swiss Center for Scientific Computing: Manno, Switzerland, 2000.

(26) Schaftenaar, G.; Noordik, J. H. *J. Comput.-Aided Mol. Des.* **2000**, *14*, 123.

(27) Foresman, J. B.; Frisch, A. *Exploring Chemistry with Electronic Structure Methods*, 2nd ed.; Gaussian Inc.: Pittsburgh, PA, 1996.

(28) $\nu(CO)_{Re}$ denotes stretching of the CO ligands attached directly to Re; ν(CO) denotes stretching of the amide CO group.

(29) Baiano, J. A.; Kessler, R. J.; Lumpkin, R. S.; Munley, M. J.; Murphy, W. R., Jr. *J. Phys. Chem.* **1995**, *99*, 17680.

(30) Mallick, P. K.; Danzer, G. D.; Strommen, D. P.; Kincaid, J. R. *J. Phys. Chem.* **1988**, *92*, 5628.

(31) Omberg, K. M.; Schoonover, J. R.; Treadway, J. A.; Leasure, R. M.; Dyer, R. B.; Meyer, T. J. *J. Am Chem. Soc.* **1997**, *119*, 7013.

(32) Okamoto, H.; Inishi, H.; Nakamura, Y.; Kohtani, S.; Nakagaki, R. *Chem. Phys.* **2000**, *260*, 193.

(33) Bellamy, L. J. *The Infrared Spectra of Complex Molecules*, 2nd ed.; Methuen and Co. Ltd.: London, 1958.

(34) Dollish, F. R.; Fateley, W. G.; Bentley, F. F. *Characteristic Raman Frequencies of Organic Compounds*; John Wiley and Sons, Inc.: New York, 1974.

(35) Tu, A. T. *Raman Spectroscopy in Biology: Principles and Applications*; John Wiley and Sons, Inc.: New York, 1982.

(36) The alkene and alkyne models we studied were -NEt_2 rather than -NMe_2 systems, and we assigned their corresponding modes to bands at 1407 cm^{-1};[7] the different behavior may arise from the mixed nature of the modes because the coupling of the methyl vibrations will be different from that of the ethyl vibrations.

(37) Guichard, V.; Bourbka, A.; Lautie, M.-F.; Poizat, O. *Spectrochim. Acta, Part A* **1989**, *45*, 187.

(38) Forster, M.; Hester, R. E. *J. Chem. Soc., Faraday Trans. 2* **1981**, *77*, 1535.

(39) Poizat, O.; Guichard, V.; Buntinx, G. *J. Chem. Phys.* **1989**, *90*, 4697.

(40) Brouwer, A. M.; Wilbrandt, R. *J. Phys. Chem.* **1996**, *100*, 9678.

(41) DFT calculated dihedral angles of +5.0° and +5.9° give two near-equivalent C(Ph)-C(Ph)-N-C(H_3) dimethylamino group geometries that indicate that the nitrogen atom is only slightly pyramidal in the ground state of L**2**.

(42) Kushto, G. P.; Jagodzinski, P. W. *Spectrochim. Acta, Part A* **1998**, *54*, 799.

(43) Chujo, T.; Saraoka, I.; Kato, S.; Sato, H.; Fukuhara, K.; Matsuura, H. *J. Inclusion Phenom. Mol. Recognit. Chem.* **1995**, *20*, 173.

(44) Del Zoppo, M.; Tommasini, M.; Castiglioni, C.; Zerbi, G. *Chem. Phys. Lett.* **1998**, *287*, 100.

(45) Kwok, W. M.; Ma, C.; Phillips, D.; Matousek, P.; Parker, A. W.; Towrie, M. *J. Phys. Chem. A* **2000**, *104*, 4188.

(46) Kwok, W. M.; Ma, C.; Matousek, P.; Parker, A. W.; Phillips, D.; Toner, W. T.; Towrie, M.; Umapathy, S. *J. Phys. Chem. A* **2001**, *105*, 984.

(47) Okamoto, H. *J. Phys. Chem A* **2000**, *104*, 4182.

(48) Okamoto, H.; Kinoshita, M.; Kohtani, S.; Nakagaki, R.; Zachariasse, K. A. *Bull. Chem. Soc. Jpn.* **2002**, *75*, 957.

(49) Chen, X. G.; Schweitzer-Stenner, R.; Asher, S. A.; Mirkin, N. G.; Krimm, S. *J. Phys. Chem.* **1995**, *99*, 3074.

(50) Wang, Y.; Purrello, R.; Jordan, T.; Spiro, T. G. *J. Am. Chem. Soc.* **1991**, *113*, 6359.

(51) Some bands of **1** show small changes in position and intensity between dichloromethane and acetonitrile solvents, as can be seen in Figures 1 and 4.

(52) Devalaux-Nicot, B.; Mayanadié, J.; Lavabre, D.; Lepetit, C.; Donnadieu, B. *Eur. J. Inorg. Chem.* **2005**, 2483.

(53) A re-examination of earlier resonance Raman spectra[3] we recorded with low-energy pulsed 385 nm excitation of **1**-M^{n+} samples at high M^{n+} concentrations in CH_3CN is consistent with this effect. The RR spectra from **1**-Na^+, **1**-Ca^{2+}, and **1**-Ba^{2+} samples showed upshifted ground-state amide I bands at ca. 1685, 1690, and 1685 cm^{-1}, respectively, that are attributable to azacrown-only binding and downshifted bands at ca. 1654, 1650, and 1655 cm^{-1} that are attributable to binding to both azacrown and amide groups. The RR spectra from **1**-Li^+ samples showed one broad feature peaking at ca. 1669 cm^{-1} that band-fitting indicates may comprise upshifted and downshifted bands at ca. 1685 and 1667 cm^{-1}, respectively.

(54) We use **1**-Ba^{2+} as a general label for samples of **1** in the presence of barium perchlorate, while noting that the samples in this particular study were actually a mixture comprising mainly **1**-Ba^{2+} (azacrown bound) and **1**-$(Ba^{2+})_2$ (azacrown and amide carbonyl bound) forms (see Discussion).

(55) Fedorova, O. A.; Maurel, F.; Chebun'kova, A. V.; Strokach, Y. P.; Valova, T. M.; Kuzmina, L. G.; Howard, J. A. K.; Wenzel, M.; Gloe, K.; Lokshin, V.; Samat, A. *J. Phys. Org. Chem.* **2007**, *20*, 469.

(56) Blanco-Rodríguez, A. M.; Busby, M.; Grădinaru, C.; Crane, B. R.; Di Bilio, A. J.; Matousek, P.; Towrie, M.; Leigh, B. S.; Richards, J. H.; Vlček, A., Jr.; Gray, H. B. *J. Am. Chem. Soc.* **2006**, *128*, 4365.

(57) Our reported TRVIS kinetics gave a rate constant of 2.0×10^9 s^{-1}.[1] The TRIR kinetic traces reported here were obtained under slightly different sample conditions but gave rate constants of $(1-2) \times 10^9$ s^{-1} that essentially match the TRVIS value.

(58) TRIR peaks may not give the exact excited-state band positions because these are difference spectra that may be attributed to overlying contributions from several strong negative bands, due to ground-state bleaches, and several strong positive bands, due to excited-state features.

(59) Experimental limitations precluded the recording of TRIR data at ca. 1400−1480 cm^{-1} from **1**-Ba^{2+}.

(60) Note that baseline drift (Figure 12) may overemphasize the decay of positive absorption bands in this region (e.g., at ca. 1686 cm^{-1}) and underemphasize the extent of bleaching recovery (e.g., at 1658 cm^{-1}).

(61) Dumon, P.; Jonusauskas, G.; Dupuy, F.; Pée, P.; Rullière, C.; Létard, J.-F.; Lapouyade, R. *J. Phys. Chem.* **1994**, *98*, 10391.

(62) Mathevet, R.; Jonusauskas, G.; Rullière, C.; Létard, J.-F.; Lapouyade, R. *J. Phys. Chem.* **1995**, *99*, 15709.

(63) Martin, M. M.; Plaza, P.; Meyer, Y. H.; Badaoui, F.; Bourson, J.; Lefèvre, J.-P.; Valeur, B. *J. Phys. Chem.* **1996**, *100*, 6879.

(64) Plaza, P.; Leray, I.; Changenet-Barret, P.; Martin, M. M.; Valeur, B. *Chem. Phys. Chem.* **2002**, *3*, 668.

(65) Marcotte, N.; Plaza, P.; Lavabre, D.; Fery-Forgues, S.; Martin, M. M. *J. Phys. Chem. A* **2003**, *107*, 2394.

(66) The DFT calculated *N*(Py)-*N*(dimethylamino) distance of L**2** was 10.7 Å (through-space).